AD-A278 288

PAGE

Form Approved
OMB No 0704-0188

1. AGENC...

3. REPORT TYPE AND DATES COVERED
Notification of Publication

4. TITLE AND SUBTITLE
"$L1_2Al_3Ti$-based Alloys with Al_2Ti Precipitates (II): Deformation Behavior of Single Crystals", Acta Met. et Mat., in press.

5. FUNDING NUMBERS
61102F 2306 AS

(2)

6. AUTHOR(S)
D. Pope and Z.L. Wu

7. PERFORMING ORGANIZATION NAME(S) AND ADDRESS(ES)
Univ of Pennsylvania
3231 Walnut Street, Suite 200
Philadelphia, PA 19104

DTIC ELECTE APR 21 1994 S F D

8. PERFORMING ORGANIZATION REPORT NUMBER
AFOSR-TR- 94 0179

9. SPONSORING/MONITORING AGENCY NAME(S) AND ADDRESS(ES)
AFOSR/NC
110 DUNCAN AVENUE SUITE B115
BOLLING AFB DC 20332-0001

10. SPONSORING/MONITORING AGENCY REPORT NUMBER
F49620-92-J-0019

11. SUPPLEMENTARY NOTES
Acta. Metall. Mater. Vol. 42, No. 2 pp 519-526

12a. DISTRIBUTION/AVAILABILITY STATEMENT
APPROVED FOR PUBLIC RELEASE; DISTRIBUTION IS UNLIMITED.

12b. DISTRIBUTION CODE

13. ABSTRACT (Maximum 200 words)

The operating slip systems and flow behavior of single crystalline $Al_{66.8}Ti_{27.4}Fe_{5.8}$, a two phase $L1_2+Al_2Ti$ material, was investigated as a function of temperatures using specimens with compressive axes near [001], [$\bar{1}$13], [$\bar{1}$12], [013] and [$\bar{1}$33]. The material shows a very limited compressive ductility, and fracture occurs by cleavage along planes of low indices, such as {011}, {001}, {013} and {111}. Slip occurs exclusively on the octahedral slip systems at low temperatures, and on both octahedral and cube systems at high temperatures. A transition in operating slip systems from octahedral slip to cube slip, similar to the one seen in Ni_3Al-type alloys, occurs as the temperature increases and as the orientation of the specimens change from near-[001] to near-[$\bar{1}$11]. The transition in slip system is attributed to the hardening effect of the Al_2Ti precipitates, rather than to the anisotropy of APB energy on cube and octahedral slip planes of the matrix. Because of the large hardening effect of the Al_2Ti, the two phase material is substantially stronger than single $L1_2$ phase materials. The shape (but not the level) of the flow stress-temperature curve for the two phase material resembles that of the single phase $L1_2$ material at low and intermediate temperatures. At high temperatures, however, the flow stress of the two phase material exhibits a sharp decrease, a feature which is not observed in the single phase $L1_2$ materials and can be correlated with a continuous dissolution of the Al3Ti precipitates at high temperatures.

94-12066

94 4 20 085

14. SUBJECT TERMS

15. NUMBER OF PAGES
8

16. PRICE CODE

17. SECURITY CLASSIFICATION OF REPORT	18. SECURITY CLASSIFICATION OF THIS PAGE	19. SECURITY CLASSIFICATION OF ABSTRACT	20. LIMITATION OF ABSTRACT
UNCLASSIFIED	UNCLASSIFIED	UNCLASSIFIED	

Acta metall. mater. Vol. 42, No. 2, pp. 519–526, 1994
Printed in Great Britain.
0956-7151/94 $6.00 + 0.00

$L1_2$ Al_3Ti-BASED ALLOYS WITH Al_2Ti PRECIPITATES—II. DEFORMATION BEHAVIOR OF SINGLE CRYSTALS

Z. L. WU and D. P. POPE
Department of Materials Science and Engineering, University of Pennsylvania, Philadelphia, PA 19104, U.S.A.

(*Received 27 May 1993*)

Abstract—The operating slip systems and flow behavior of single crystalline $Al_{66.8}Ti_{27.4}Fe_{5.8}$, a two phase $L1_2 + Al_2Ti$ material, was investigated as a function of temperatures using specimens with compressive axes near [001], [$\bar{1}$13], [$\bar{1}$12], [013] and [$\bar{1}$33]. The material shows a very limited compressive ductility, and fracture occurs by cleavage along planes of low indices, such as {011}, {001}, {013} and {111}. Slip occurs exclusively on the octahedral slip systems at low temperatures, and on both octahedral and cube systems at high temperatures. A transition in operating slip systems from octahedral slip to cube slip, similar to the one seen in Ni_3Al-type alloys, occurs as the temperature increases and as the orientation of the specimens change from near-[001] to near-[$\bar{1}$11]. The transition in slip system is attributed to the hardening effect of the Al_2Ti precipitates, rather than to the anisotropy of APB energy on cube and octahedral slip planes of the matrix. Because of the large hardening effect of the Al_2Ti, the two phase material is substantially stronger than single $L1_2$ phase materials. The shape (but not the level) of the flow stress–temperature curve for the two phase material resembles that of the single phase $L1_2$ material at low and intermediate temperatures. At high temperatures, however, the flow stress of the two phase material exhibits a sharp decrease, a feature which is not observed in the single phase $L1_2$ materials and can be correlated with a continuous dissolution of the Al_2Ti precipitates at high temperatures.

INTRODUCTION

In searching for new high strength materials for aerospace applications, a great deal of attention has been recently given to three intermetallics in the Ti–Al system: Ti_3Al, TiAl and Al_3Ti. These alloys have relatively high melting temperatures and low densities since they are composed of two light elements. However, brittleness is the major barrier to practical use of these materials. Among the three titanium aluminides, Ti_3Al and TiAl have already been studied in great detail. Of the three, Al_3Ti contains the largest fraction of aluminium, and as a result, has the lowest density (~ 3.3 g/cm^3) and best oxidation resistance. The surface of Al_3Ti is composed of Al_2O_3, which acts as a highly effective barrier against oxygen diffusion [1], while the oxide films formed on Ti_3Al and TiAl are TiO_2 and a mixture of TiO_2 and Al_2O_3, respectively [2, 3]. In stoichiometric form Al_3Ti has the DO_{22} tetragonal crystal structure. Studies of the deformation of binary Al_3Ti started with the work of Yamaguchi and coworkers [3–5]. These investigators found that the deformation modes are temperature dependent: at low temperatures, deformation is carried by twinning on octahedral planes, while at high temperatures, both twinning and cube slip contribute. They suggested that one way to improve the ductility of Al_3Ti is to alloy it with elements which enhance the activation of ordered twinning and/or cube slip. Elements such as Zr and Hf have been found to improve the ductility to some extent by causing cube slip [4], but no substantial improvement has been achieved so far.

A possible alternative approach to the above-mentioned methods of improving ductility is to transform the DO_{22} structure of Al_3Ti into the high symmetry f.c.c.-based $L1_2$ structure via appropriate alloying. Such a transformation might possibly cause an improvement in ductility by increasing the number of available slip systems. A number of elements, such as Cr, Mn, Fe, Ni, Cu, Zn, Pd and Ag, are known to promote the DO_{22} to $L1_2$ transition [6–16]. According to the work of Mazdiyasni *et al.* [11], the single phase $L1_2$ fields at 1200°C in the Al–Ti–X (where X = Fe, Ni and Cu) ternary systems have widths of approximately 7, 4 and 11.5 at.%, respectively. However, the size of the $L1_2$ phase field shrinks between 1200 and 800°C, and the shrinkage is not concentric but skews towards the Al-rich corner. Our previous study of the Al–Ti–Fe ternary system has shown that the shrinkage continues at even lower temperatures, and at room temperature the single phase $L1_2$ field appears to vanish [17]. Five different second phases are found to be in equilibrium with the $L1_2$ matrix, depending on overall compositions. Among the five second phases, Al_2Ti has the largest effect on the mechanical properties. A detailed study of the temperature- and composition-dependent stability of the Al_2Ti has been presented in the accompanying paper [18]. In this paper the effect of Al_2Ti on the deformation behavior of the $L1_2$ Al_3Ti-based alloys is described.

Approved for public release; distribution unlimited.

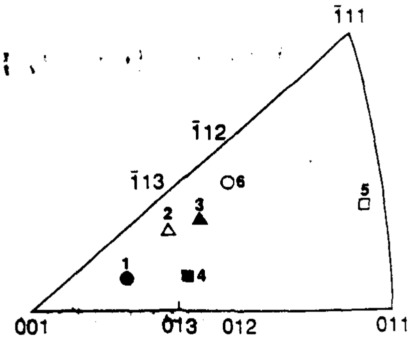

Fig. 1. The orientations of the single crystalline specimens used in this study.

EXPERIMENTAL

A single crystal of nominal composition $Al_{66}Fe_6Ti_{28}$ was produced using the same procedure described in [18]. The distribution and composition of phases in the crystal were checked using X-ray powder diffraction and fully quantitative energy dispersive spectroscopy in an SEM. Specimens of dimension $3 \times 3 \times 5$ mm with compressive axes near [001], [013], [113], [112] and [133] (Fig. 1) were cut using an electron discharge machine and then abraded on grade 600 SiC paper. The two orthogonal faces were subsequently metallographically polished and the specimens were then annealed for two hours to remove the surface strain induced by the mechanical polishing and then cooled to room temperature at a rate of about 65°C/h. The two orthogonal faces were given a final polishing for later operating slip system analysis. Compression tests were performed on an Instron Universal Testing Machine at temperatures between 77 K and 1300 K, at a nominal strain rate of about $1.7 \times 10^{-4}\ s^{-1}$ (unless otherwise noted).

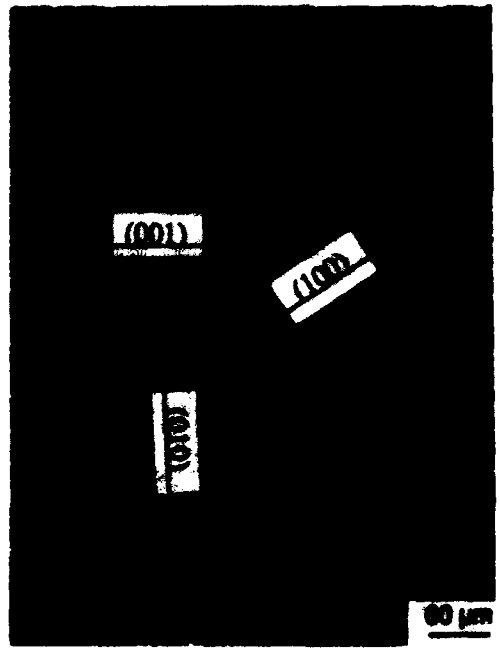

Fig. 2. A surface of a single crystalline specimen after being polished and chemcally etched, where the Al_3Ti platelets are easily seen to form on {100} planes.

The operating slip systems were identified using two-surface slip trace analysis in an optical microscope equipped for Nomarski interference contrast.

RESULTS AND DISCUSSIONS

The as-grown crystal is of overall composition $Al_{66.8}Ti_{27.4}Fe_{5.8}$, with an $L1_2$ matrix and a large volume fraction of second phase Al_3Ti. Figure 2

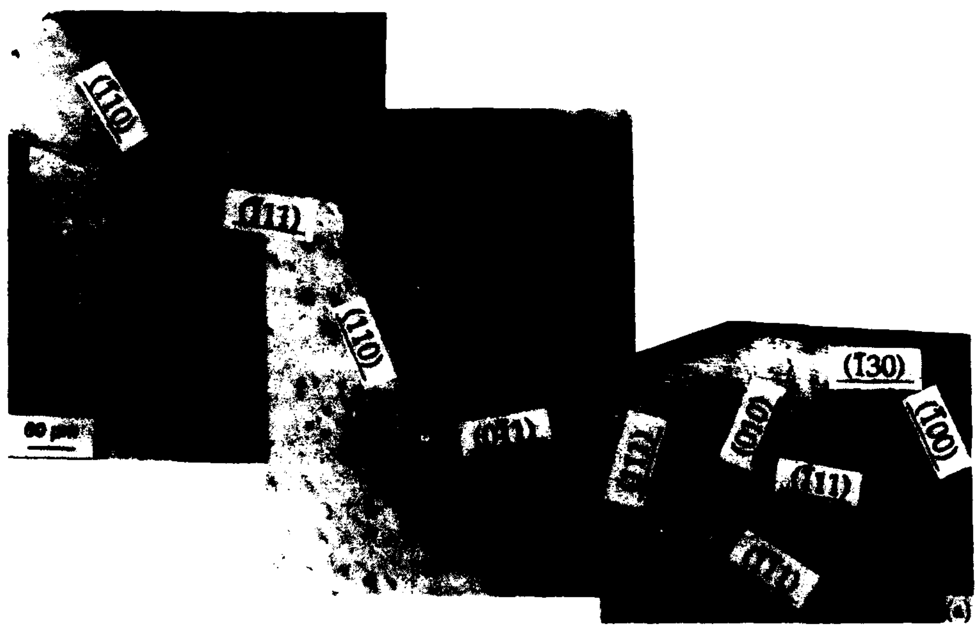

Fig. 3(a). *Caption on facing page.*

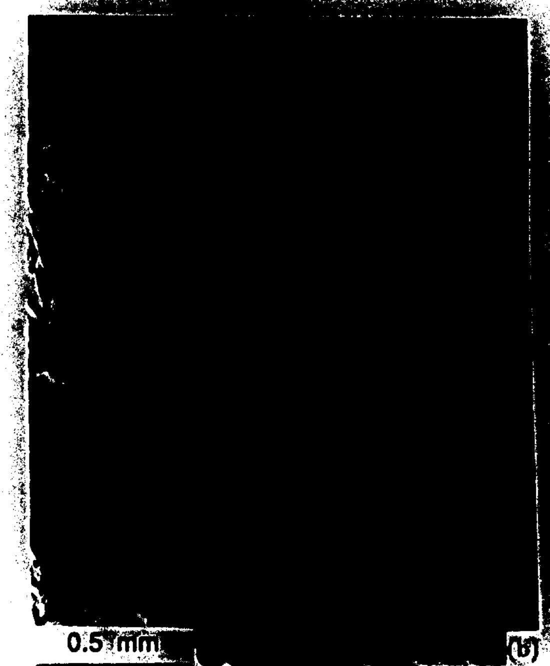

Fig. 3. (a), (b) show, respectively, a side and a top view of a fractured single crystalline sample tested at a strain rate about $1.7 \times 10^{[illegible]}$ s^{-1} at 770°C.

shows a surface of a single crystalline specimen after being mechanically polished and chemically etched (using the etching solution shown in Table 2 in [18]), where the Al_3Ti platelets are seen to form in a three dimensional dense array on {100} planes. The volume fraction of the phase is estimated to be about 29% [18]. In addition to the Al_3Ti, a small amount of ribbon-like Ti_2NAl precipitates (< 1 vol.%) is also observed.

The single crystal was found to be even more brittle than polycrystals of the same composition. Small cracks were often seen on the surfaces of the single crystalline specimens after only 0.2% compressive plastic deformation, while the polycrystalline specimens of the same composition could be deformed plastically to 1.5% strain. The brittleness probably results from the fact that cleavage is relatively easier in the single crystal and the second phase precipitates embrittle. Figure 3 shows a fractured single crystalline sample tested at a strain rate about $1.7 \times 10^{[illegible]}$ s^{-1} at 770°C. Although one cube and three octahedral slip systems were activated near the fracture surfaces, the specimen failed in a brittle manner by cleavage along {110}, {001}, {013} and {111} planes, as determined using single surface trace analysis (assuming that cleavage occurs on low index planes). The observation agrees well with the results of George *et al.* [19]. Note that the cleavage surfaces change continuously from one type to the other in Fig. 3(a), and cracks pass smoothly across the matrix precipitate interfaces, indicating that these planes are nearly equally brittle, as are the matrix and the Al_3Ti precipitates. Although the ribbon-like Ti_2NAl precipitates constitute only a small volume fraction, they severely embrittle the material (see Fig. 4). It has been seen in a separate study that the ribbon-like Ti_2NAl precipitates contain internal

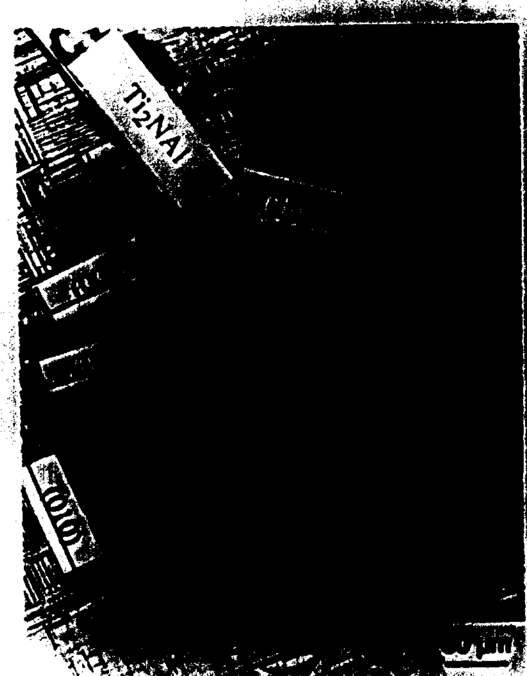

Fig. 4. A crack is seen to initiate at the interface between a Ti_2NAl precipitate and the matrix in a single crystalline specimen after plastic deformation to 0.2% strain at room temperature. Also observed are slip bands of {111}-type and Al_3Ti platelets on {100} planes.

cracks which are formed during processing prior to mechanical deformation, and in addition the interfaces between the precipitates and the matrix are particularly weak [20]. Therefore, cracks can easily nucleate and propagate within the precipitates and/or along the interfaces. The Al_2Ti, on the other hand, does not seem to embrittle the material directly by providing sites for crack initiation. However, the phase has a large hardening effect (as will be discussed later) which can indirectly affect the ductility of the material by substantially increasing the flow stress.

The operating slip systems seen in the specimens with compressive axes near [001], $[\bar{1}12]$, [013] and [133] tested at elevated temperatures were analyzed [Fig. 5(a–d)]. The Al_2Ti phase is not visible in Fig. 5 since the surfaces of the specimens were not chemically etched. The slip bands seen in all the deformed specimens are coarse, unevenly distributed, and limited in number. In comparison, the slip lines previously seen in nearly single phase $L1_2$ materials, $Al_{67}Fe_8Ti_{25}$ and $Al_{67}Cr_8Ti_{25}$, were fine dense, and evenly distributed across the entire surface of the

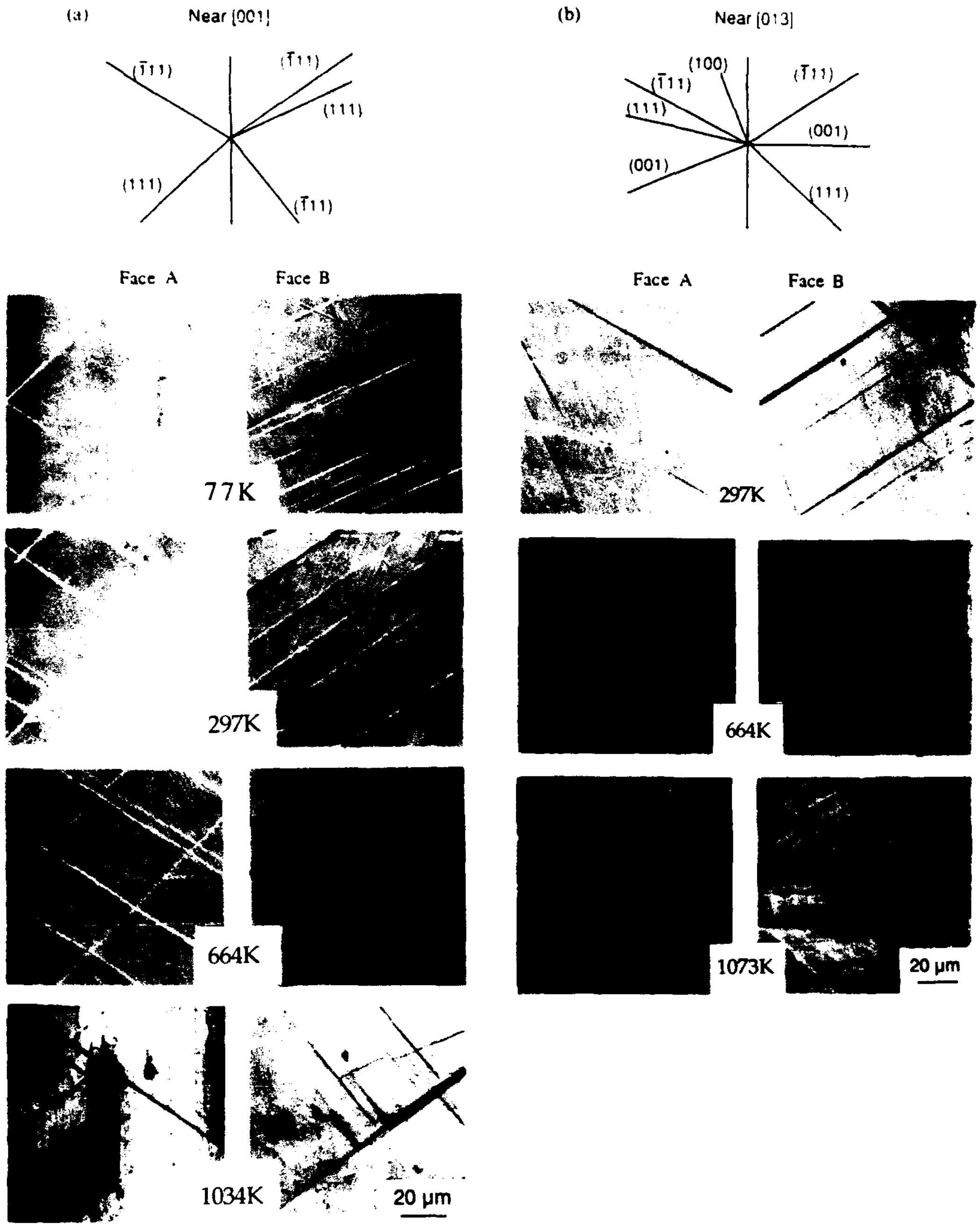

Fig. 5(a,b). *Caption on facing page.*

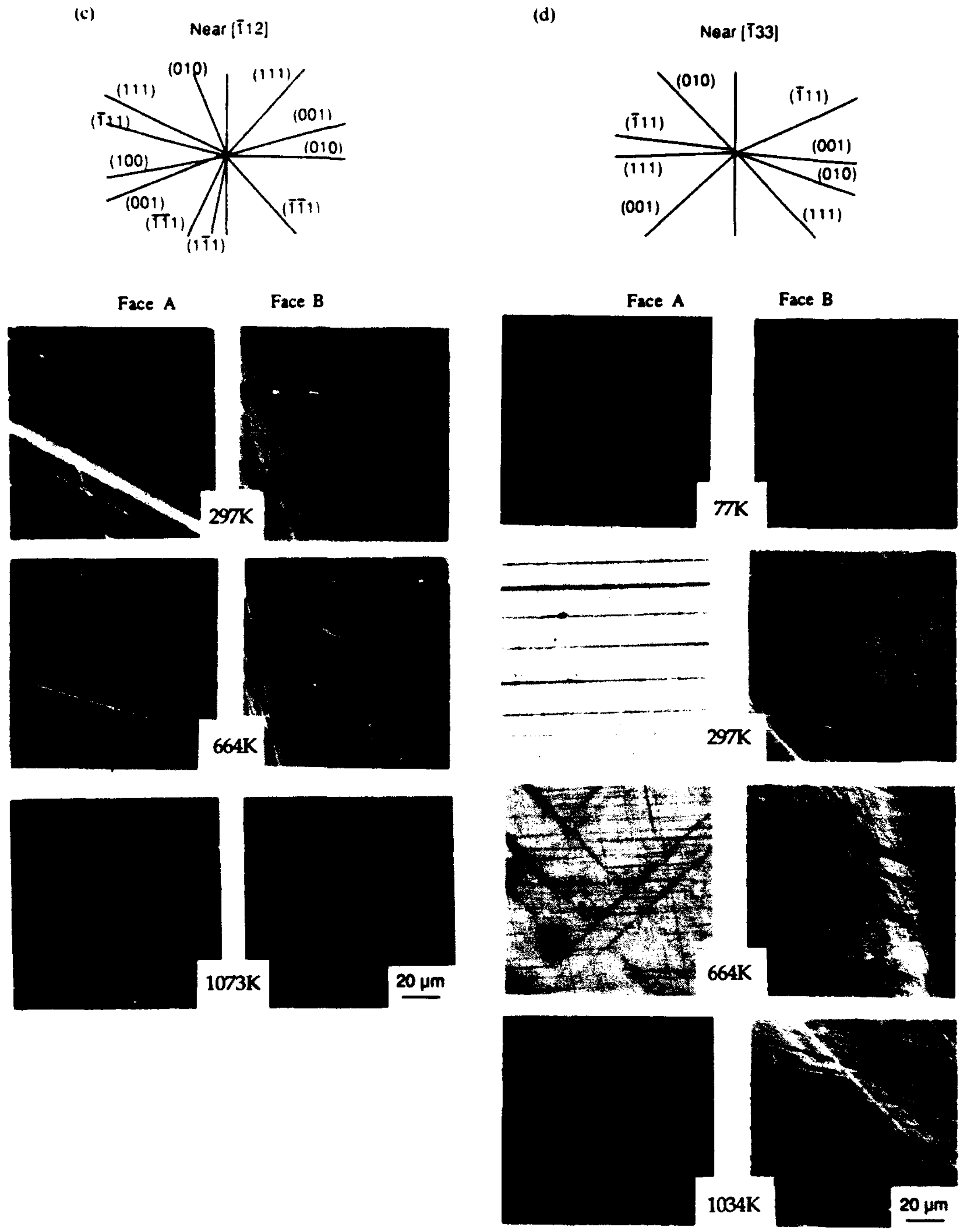

Fig. 5. The operating slip systems observed in specimens of the orientations indicated. Details are discussed in the text.

deformed specimens [21, 22]. In the two phase specimens with compressive axes near [001] and [013], the operating slip systems at all temperatures are predominantly octahedral, although some cube slip lines are also seen at high temperatures. For these two orientations the Schmid factor for cube slip is substantially smaller than for octahedral slip (see Table 1). In specimens orientated near [$\bar{1}$12] and [$\bar{1}$33], the Schmid factors for cube and octahedral slip are comparable, however, only octahedral slip is observed at low temperatures. But as the temperature is increased, both octahedral and cube slip are activated, and in the near-[$\bar{1}$33] specimen the number of cube slip lines at high temperatures exceeds the

Table 1. Schmid factors on the major slip systems for single crystalline specimens of four different orientations

Orientations	$[\bar{1}01](111)$	$[101](\bar{1}11)$	$[011](\bar{1}\bar{1}1)$	$[1\bar{1}0](001)$	$[\bar{1}01](010)$
1	0.476	0.463	0.405	0.199	0.158
2	0.482	0.436	0.410	0.323	0.242
3	0.483	0.418	0.390	0.373	0.292
4	0.497	0.473	0.349	0.288	0.252
5	0.445	0.326	0.162	0.447	0.437
6	0.461	0.360	0.385	0.433	0.340

number of octahedral slip lines [Fig. 5(c, d)]. Such a transition in slip system from octahedral-type to cube-type as the temperature is increased and as the compressive axis is moved from [001] towards $[\bar{1}11]$ in the standard unit triangle, has been commonly observed in $L1_2$ Ni_3Al-type alloys [23], and is explained in terms of anisotropy of the APB energy on cube and octahedral slip planes of the matrix, as well as a decreasing Peierls stress for cube slip as the temperature is increased [24]. In the material studied here, however, the transition is much more gradual than in Ni_3Al, and is probably not intrinsic to the $L1_2$ matrix since it was not observed in nearly single phase $Al_{67}Fe_8Ti_{25}$ and $Al_{67}Cr_8Ti_{25}$ [21, 22]. In fact, since the transition only occurs in samples containing relatively high Ti contents and large volume fractions of Al_2Ti precipitates, it is probably related to the precipitates themselves. Although octahedral slip is favored in single phase $L1_2$ Al_3Ti-based alloys at all deformation temperatures, it is probably not favored in the Al_2Ti precipitates because of their complex tetragonal structure and therefore the CRSS is high for slip on {111} in the two phase samples. Two possible reasons may account for the cube slip at high temperatures: (1) ⟨110⟩ superdislocations have been seen to dissociate on cube planes of the $L1_2$ matrix only at high temperatures [25–27]. Due to their sessile core structures [28] these dislocations are difficult to move in single phase materials where octahedral slip can be activated at relatively lower stresses. However, in two phase materials octahedral slip is inhibited by the precipitates and the flow stress is then high enough to activate the cube slip in the matrix. (2) The deformation modes in the Al_2Ti precipitates at high temperatures may encourage cube slip when the stress level is high, as in (1). At high volume fractions of Al_2Ti the slip plane of the composite sample may be determined by the properties of both the matrix ({111} slip) and the precipitates ({010}) slip near

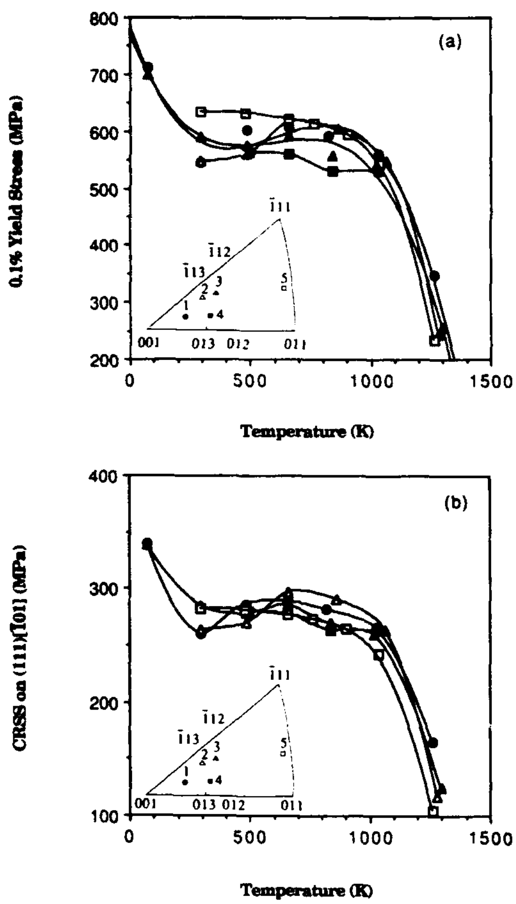

Fig. 6. (a, b) The flow stress and corresponding CRSS on $[\bar{1}01](111)$ as functions of temperature and orientation. Note the yield stresses are measured at 0.1% instead of the 0.2% offset plastic strain since small cracks often occur after 0.2% plastic strain. Note also that Schmid's law is obeyed.

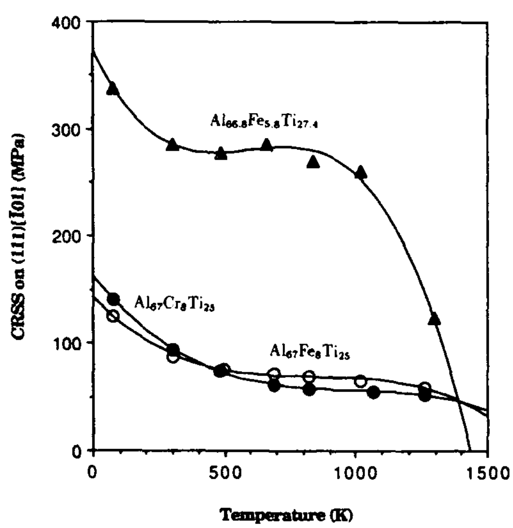

Fig. 7. A comparison of flow behaviors of single crystalline specimens having compositions $Al_{66.8}Fe_{5.8}Ti_{27.4}$, $Al_{67}Fe_8Ti_{25}$ and $Al_{67}Cr_8Ti_{25}$.

[$\bar{1}11$]. Such a hypothesis can be tested by analyzing the deformation modes in a single phase Al_3Ti alloy, but that is beyond the scope of the present study.

Figure 6(a) and (b) show the flow stress and corresponding CRSS as functions of temperature and orientation. Here the yield stresses are measured at 0.1% instead of the more usual 0.2% offset plastic strain, since small cracks often occurred after 0.2% plastic strain. The differences in CRSS for specimens of different orientations are very small, implying that Schmid's law is obeyed by this material. The material is very strong with a CRSS around 275 MPa at room temperature. In comparison, the CRSS for the near-single phase $Al_{67}Fe_8Ti_{25}$ and $Al_{67}Cr_8Ti_{25}$ (at 0.2% plastic strain) are only about 90 and 85 MPa, respectively. Generally, the yield stress and the CRSS of the two phase samples are relatively constant in the intermediate temperature range, but decrease rapidly with temperature at low and high temperatures. This feature of the flow behavior is similar to that of the near single phase $Al_{67}Fe_8Ti_{25}$ and $Al_{67}Cr_8Ti_{25}$ (see Fig. 7), except at temperatures higher than 750 C where the Al_3Ti precipitates start to dissolve and the CRSS drops more rapidly than for the near-single phase material. The CRSS vs temperature behavior of the single phase $L1_2$ samples and the $L1_2 + Al_3Ti$ samples are explained in the following way: in the single phase samples, the $\langle\bar{1}01\rangle$ superdislocations are dissociated into two $\langle 112\rangle/3$ dislocations separated by SISF at low temperatures [21, 29]. Since these dislocations are expected to have a nonplanar core, motion at low temperatures is thermally activated, leading to the sharp drop in CRSS with increasing temperature. At intermediate and high temperatures the dissociations dissociate into two $\langle 101\rangle/2$ superpartials separated by APB, which have planar cores. Since the cores are planar, thermal activation is not required and the CRSS is roughly temperature-independent. In the two phase material, the same temperature dependence (but a higher level) is seen at low temperatures, again because of the nonplanar cores. The CRSS then drops to the athermal level necessary to drive dislocations through the Al_3Ti platelets and remains at that relatively high level until the precipitates dissolve, leading to a dramatic drop in CRSS. Thus the flow stress–temperature curve of the two phase material is the same as that of the single phase material, but uniformly shifted to higher stress levels (except at high temperatures where the precipitates dissolve). We therefore conclude that the hardening is not due to a change in dislocation structure as suggested by Potez *et al.* [30], but is simply the result of dislocation-precipitate interactions.

CONCLUSIONS

Two phase single crystalline $L1_2$ $Al_{66.8}Fe_{5.8}Ti_{27.4}$ is very brittle. The brittleness is caused by cleavage on {001}, {011}, {013} and {111} planes. A small amount of Ti_2NAl further embrittles the material. Plastic deformation in the alloy is carried by octahedral slip at low temperatures and by both cube and octahedral slip at high temperatures. A transition in slip mode from octahedral-type to cube-type occurs as the temperature increases and as the orientation of the specimen changes from near-[001] to near-[$\bar{1}11$], and has been correlated to the hardening effect of the Al_3Ti. The flow behavior of the two phase material is controlled by both the core configurations of the $\langle 110\rangle\{111\}$ superdislocations and the hardening effect of the Al_3Ti precipitates. The flow stress decreases rapidly with temperature at low temperatures and is athermal at intermediate temperatures, due to a change in the cores of the superdislocations from nonplanar (sessile) at low temperatures to planar (glissile) at intermediate temperatures. The effect of the Al_3Ti is simply additive in this temperature range (since thermal activation does not assist in dislocation penetration of the precipitates). The flow stress at high temperatures decreases sharply as the Al_3Ti continuously dissolves.

Acknowledgements—This work was supported by the AFOSR under Grant AFOSR-92-J0019. Research facilities were provided by the LRSM supported by the NSF MRL program under Grant DMR-91-20668. The authors wish to thank W. J. Romanow and R. Hsiao for experimental assistance.

REFERENCES

1. K. Hashimoto, T. Tsujimoto and H. Doi, *Japan J. Inst. Metals* **49**, 410 (1985).
2. M. Kablaj, A. Galerie and M. Caillet, *J. less-common Metals* **A108**, 1 (1985).
3. M. Yamaguchi, Y. Umakoshi and T. Yamane, *Phil. Mag. A* **55**, 301 (1987).
4. M. Yamaguchi, Y. Shirai and Y. Umakoshi, *Dispersion Strengthened Aluminum Alloys*, p. 721. TMS, Warrendale, Pa (1988).
5. M. Yamaguchi and Y. Umakoshi, *Prog. Mater. Sci.* **34**, No. 1 (1990).
6. H. Mabuchi, K. Hirukawa and Y. Makayama, *Scripta metall.* **23**, 1761 (1989).
7. H. Mabuchi, K. Hirukawa, H. Tsuda and Y. Makayama, *Scripta metall. mater.* **24**, 1553 (1990).
8. S. Zhang, J. P. Nic, W. W. Milligan and D. E. Mikkola, *Scripta metall. mater.* **24**, 57 (1990).
9. J. P. Nic, S. Zhang, D. E. Mikkola, *Scripta metall. mater.* **24**, 1099 (1990).
10. K. S. Kumar and J. R. Pickens, *Dispersion Strengthened Aluminum Alloys* (edited by Y.-W. Kim and W. Griffith), p. 763. TMS, Warrendale, Pa (1988).
11. S. Mazdiyasni, D. B. Miracle, D. M. Dimiduk, M. G. Mendiratta and P. R. Subramanian, *Scripta metall.* **223**, 327 (1989).
12. K. Schubert, H. G. Meissner, A. Raman and W. Rossteutscher, *Naturwissenschaften* **51**, 287 (1964).
13. K. Schubert, H. G. Meissner and W. Rossteutscher, *Naturwissenschaften* **51**, 507 (1964).
14. A. Raman and K. Schubert, *Z. Metallk.* **56**, 99 (1965).
15. A. Raman and K. Schubert, *Z. Metallk.* **56**, 40 (1965).
16. W. O. Powers and J. A. Wert, *Metall. Trans.* **21A**, 145 (1990).
17. Z. L. Wu, D. P. Pope and V. Vitek, *MRS Symp. Proc.* **288**, 367 (1993).

18. Z. L. Wu and D. P. Pope, *Acta metall. mater.* **42**, 509 (1994).
19. E. P. George, W. D. Porter, H. M. Henson, W. C. Oliver and B. F. Oliver, *J. Mater. Res.* **4**, 78 (1989).
20. Z. L. Wu and D. P. Pope, *Metall. Trans.* Submitted.
21. Z. L. Wu Ph.D thesis, The Univ. of Pennsylvania (1992).
22. Z. L. Wu, D. P. Pope and V. Vitek, *MRS Symp. Proc.* **288**, 447 (1993).
23. C. Lall, S. Chin and D. P. Pope, *Metall. Trans.* **10A**, 1323 (1979).
24. D. P. Pope and S. S. Ezz, *Int. Metals Rev.* **29**, 136 (1984).
25. V. Vansudevan, R. Wheeler and H. L. Fraser, *High Temperature Ordered Intermetallic Alloys* (edited by C. T. Liu, A. I. Taub, N. S. Stoloff and C. C. Koch), Vol. 133, p. 705. MRS, Pittsburgh, Pa (1989).
26. R. Lerf and D. G. Morris, *Acta metall. mater.* **39**, 9 (1991).
27. H. Inui, D. E. Luzzi, W. D. Porter, D. P. Pope, V. Vitek and M. Yamaguchi, *Phil. Mag. A* **65**, 245 (1992).
28. V. Vitek, M. Khantha, J. Cserti and Y. Sodani, *Proc. JIMIS-6* (1991).
29. Z. L. Wu and D. P. Pope, *Int. Symp. on Structural Intermetallics*, Seven Springs, Champion, Pa (1993).
30. L. Potez, A. Loiseau, S. Naka and G. Lapasset, *J. Mater. Res.* **7**, 876 (1992).